



Self-healing capability of conventional, high-performance, and Ultra High-Performance Concrete with commercial bacteria characterized by means of water and chloride penetration

Hesam Doostkami^{a,*}, Javier de Jesús Estacio Cumberbatch^a, Sidiclei Formagini^b, Pedro Serna^a, Marta Roig-Flores^c

^a Universitat Politècnica de València, Instituto de Ciencia y Tecnología del Hormigón, Valencia, Spain

^b Universidade Federal de Mato Grosso do Sul, FAENG – Faculdade de Engenharias, Arquitetura e Urbanismo e geografia, Campo Grande, Brazil

^c Universitat Jaume I, Department of Mechanic Engineering and Construction, Castelló de la Plana, Spain

ARTICLE INFO

Keywords:

Self-healing
Crack closing
Water permeability
Chloride penetration
High-performance concrete
Ultra High-Performance Concrete

ABSTRACT

This study analyzes the self-healing capability of conventional, High-Performance, and Ultra High-Performance Concrete specimens, incorporating commercial bacteria products that are easily accessible, marketed, and affordable from different sectors. Bacteria were incorporated into different mediums: immobilized in diatomaceous earth and liquid. Specimens were pre-cracked to a range of 50–450 μm cracks and were left to heal for 28 days in 3 different conditions (1) water immersion, 2) one week of water immersion followed by three weeks in a humidity chamber, and 3) humidity chamber. To evaluate the self-healing enhancements of specimens using a bacteria-based healing agent, self-healing efficiency was quantified by optical assessment of crack closure, recovery of water tightness via water permeability testing, and chloride permeability via cracks and matrix. The results show that bacterial agents increased the protection against chloride penetration in cracked and healed specimens of conventional concrete, especially when the specimens were healed in water immersion. Owing to the dense matrix of HPC and UHPC, the chloride penetration in the presence of cracks up to 400 μm can be kept below 10 mm. Crack closure greater than 50% is required in UHPC samples to get a significant healing ratio. The penetration through the cracks is approximately twice that of the matrix penetration in conditions when healing is not enhanced.

1. Introduction

Cracks in concrete may reduce the durability of concrete structures since they open a path for aggressive agents, substantially contributing to increasing the permeability of the concrete [1,2]. According to structural codes like Model code 2010, Eurocode 2, 1992, or BS 8110–1,1997[3,4], cracks up to 300 μm are allowed depending on the environmental condition unless specific requirements like water tightness must be met. Nevertheless, not all initial cracks progress into harmful or unstable cracks. Autogenous healing of concrete is the capability to seal its own crack under certain circumstances [5–7]. This phenomenon is mainly produced by the hydration of un-hydrated cement particles and the precipitation of calcium carbonate, which is reported to be the most substantial factor influencing autogenous

healing [5,6]. The main consequence of the healing on properties would be the crack closure [8–11], durability properties, such as water permeability [12,13], and mechanical properties [8–10,14]. Various healing agents have been proposed to enhance the self-healing capacity of concrete, and most of them are chemically based [15,16]. Microbially induced calcium carbonate precipitation (MICP) has been suggested as environmentally friendly, economical and more compatible with the concrete matrix [17]. This technology is used to remove chemicals from water waste [18], bioremediation of contaminated soils [19], etc. Bacterially induced CaCO_3 precipitation is also proposed to improve the durability of the cementitious material [20–22], by healing or sealing cracks which cause a decrease in the permeability and penetration of aggressive corrosion promoters [23].

Although the direct application of the bacteria in cementitious

* Corresponding author at: ICITECH – Institute of Concrete Science and Technology, Edificio 4N, Universitat Politècnica de València, Camino de Vera, s/n 46022 Valencia, Spain.

E-mail address: hedoo@doctor.upv.es (H. Doostkami).

<https://doi.org/10.1016/j.conbuildmat.2023.132903>

Received 28 February 2023; Received in revised form 13 July 2023; Accepted 7 August 2023

Available online 11 August 2023

0950-0618/© 2023 The Author(s). Published by Elsevier Ltd. This is an open access article under the CC BY-NC-ND license (<http://creativecommons.org/licenses/by-nc-nd/4.0/>).

material proposed enhances compressive strength and reduces pore volume [24], unprotected bacteria are maybe inefficient to remain viable in the harsh alkaline environment of cementitious material for a long time [25–27]. Jonkers et al. observed calcium carbonate crystals in young concrete samples (7-day-old) but not in those of 28-day [28,29]. The viability of bacteria directly embedded in the concrete matrix was reported to be restricted to about two months [28,30]. Furthermore, bacteria cells could be damaged during the mixing stage, setting, and hardening of the cementitious composite due to a decrease in micropore size in a hydration process which can crush the bacteria spores inside the pore [20,26,29,31]. To ensure the bacteria's viability, immobilization or encapsulation of the bacteria in a protective carrier is recommended [31].

Diatomaceous earth (DE) is a type of mineral siliceous compound, the product of fossilized diatoms formed in the shell of microorganisms, with high porosity and low-density structure which makes it appropriate for immobilization. Research reported that Ureolytic activity under extremely high pH reduced the viability of bacteria to 1 day while DE-immobilized bacteria showed ureolytic activity even after 2 weeks [31]. DE has been used for in-situ bioremediation of soil and groundwater [32], and due to the low heat conductivity [33] it is also used in fireproof cement and insulation materials [34]. Because of requiring a microenvironmental area for bacteria in which the local pH around the bacteria is not as high as in cement slurry, DE-immobilized bacteria can keep a certain degree of ureolytic activity in an extremely high pH environment [35]. An increase in the amount of DE introduced inside concrete can increase ureolytic activity, though the addition of DE higher than 5% of cement weight caused dry and low workable concrete mix [31]. Bacteria can also be introduced into cementitious materials in a liquid medium incorporating bacteria cells with nutrients and growth composites considering this water as a part of the required water for the concrete mix [36–38].

Crack widths considered healable by autogenous healing remain in the range of 100 to 300 μm [2,5,7,39,40]. Concrete mixtures containing encapsulated bacteria have shown a higher healing capability of 500 μm cracks under wet-dry cycles conditions [20] and a 48–80% crack healing ratio with a maximum healed crack width of 970 μm under water-immersion conditions, while the reference series presented 18–50% of crack healing ratio with a maximum healed crack width of 250 μm [41]. Moreover, no healing was observed in the samples healed in 95% relative humidity, demonstrating water's importance for triggering the healing reactions even when using bacteria as self-healing agents. This same study shows permeability results after cracking and healing, and specimens with nutrients and microencapsulated bacterial spores had a higher decrease in permeability than reference specimens, decreasing the permeability coefficient by 10 times [41].

Other studies show that the maximum healable crack width observed in pre-cracked samples with bacteria immobilized in lightweight aggregates was 610 μm , while the direct addition of *Bacillus Subtilis* showed crack healing of cracks up to 370 μm [42]. Mortar specimens using *Bacillus sphaericus* bacteria immobilized in diatomaceous earth (DE) presented partial or complete crack healing of 150 to 170 μm [31]. In other studies on mortars containing bacteria immobilized in porous expanded clay, the maximum healable crack width was twice the size (460 μm) of that in control specimens (180 μm) [43]. Likewise, hydrogel-encapsulated bacteria spores demonstrated a 68% decrease in water permeability after healing, compared to a 15 to 50% reduction for the reference samples [20].

Crack healing has been reported to reduce the water permeability and water tightness, which does not necessarily imply that a healed crack would be able to protect from chloride penetration. The amount of chloride ion ingress into uncracked concrete mainly relies on the internal pore structure of concrete. In contrast, reducing chloride permeability depends on improving the packing density of material particles [44,45]. Conventional concrete cracks smaller than 60 μm can be healed and protected against chloride penetration [46,47]. A crack width of 10

μm is critical to avoid chlorides' penetration in a structure [48,49]. In UHPFRC, chloride penetration is more dependent on the length of the healing period, according to one study [11]. Improving the aggregate-cement interface due to bacteria precipitation also reduces chloride penetration [50]. It has been reported that concrete samples incorporating *Sporosarcina pasteurii* showed reduced chloride permeability compared to samples, indicating higher durability of the cementitious material [51].

This study aims to evaluate the effect of bacteria-based commercial products on the self-healing capacity of conventional, high-performance, and ultra-high-performance concrete samples. These bacteria-based commercial products are available in large quantities in the market are affordable, and have been obtained from industries other than the construction sector. Self-healing has been characterized by the visible closure of cracks, the water permeability through cracks, and the chloride permeability through cracks and concrete matrix.

2. Research significance

There are some restrictions on the application of MICP as a self-healing technique in cementitious materials, including market availability, accessibility in large quantities, medium preparation, and economic concerns. Using bacteria-based self-healing concrete using commercial bacteria obtained from other sectors could reduce the cost of self-healing techniques, as well as restorations and maintenance applications. The findings of this study could inform the construction industry regarding the applicability and viability of using self-healing concrete with commercial bacteria in actual construction projects and ultimately contribute to the understanding of experimental techniques designed to lengthen the service life and reduce the environmental impact of concrete structures. In addition, there is no standard for evaluating concrete self-healing. Permeability tests in conventional and fiber-reinforced concrete have been extensively used to evaluate self-healing capabilities. Regarding permeability, comparing test results and testing methods for conventional concrete and UHPC concrete is still challenging, as the permeability coefficient of uncracked UHPC is below the limit of detection in several methodologies [52,53].

3. Materials and methodology

3.1. Materials and mix designs

This work studies three different types of concrete: a reference mix of conventional concrete (C30/37) labeled CC, a High-Performance Concrete (C70/85) labeled HPC, and an Ultra High-Performance (160) concrete labeled UHPC. Additionally, enhanced versions of CC, HPC, and UHPC containing three bacterial products are also studied, which will experience a combination of autogenous healing and healing produced by the bacteria.

Table 1 shows the mix design for CC and HPC mixes, and Table 2 shows the mix design for UHPC mixes. The binder components were cement CEM I 42.5 R-SR5 from Lafarge and un-densified micro-silica fume from Elkem. The limestone aggregates used in the CC and HPC mixes were 0/2 and 0/4 natural sand ($d_{\text{min}}/D_{\text{Max}}$) and crushed 7/10 and 12/20 gravels. In UHPC, silica sand of maximum sizes of 1.6 mm and 0.5 mm and silica flour were used. Superplasticizer ViscoCrete 5970 from Sika was used in CC, reference HPC mixes and HPC mixes with liquid bacteria, and ViscoCrete-20 HE in HPC mixes with bacteria in DE and UHPC to obtain targeted workability.

Moreover, to control and maintain crack opening during the pre-cracking and healing stages, all mixes incorporated 40 kg/m^3 of steel fiber Dramix 65/35 3D from Bekaert ($L = 35 \text{ mm}$, $\Phi = 0.55 \text{ mm}$, and $L/\Phi = 65$). UHPC contained the same quantity of Dramix steel fibers to ensure the formation of single cracks. Hence, the self-healing effect can be investigated by comparing the differences created by the various concrete matrices in all mixtures with comparable crack widths.

Table 1
Mix designs of Conventional and High Performance concrete.

kg / m ³	CC	CC7.5DE	CC15DE	CC25LB	HPC	HPC7.5DE	HPC15DE	HPC25LB
Cement I 42.5 R-SR	280	280	280	280	400	400	400	400
Silica Fume					40	40	40	40
Water	185	187	188	139	170	171.5	173	127.5
w/c	0.66	0.66	0.67	0.66*	0.43	0.43	0.43	0.43*
w/b	0.66	0.66	0.67	0.66*	0.39	0.39	0.39	0.39*
Sand 0/2	449	442	434	449	310	302.5	295	310
Sand 0/4	535	535	535	535	549	549	549	549
Gravel 8/16	852	852	852	852	875	875	875	875
Dramix 65/35	40	40	40	40	40	40	40	40
Superplasticizer Sika 5970	2.3	5	10	2.3	3.8			3.8
Superplasticizer Sika 20 HE						2.7	5.4	
Serenade Max		7.5	15			7.5	15	
SerBiotech				46.3				42.5

*Note: Water amount considered in water-cement and water-binder ratio evaluation includes the added water and the water in liquid bacteria (SerBiotech).

Table 2
Mix designs of Ultra High Performance concrete.

kg / m ³	UHPC	UHPC7.5DE	UHPC15DE	UHPC25LB
Cement I 42.5 R-SR	800	800	800	800
Silica Fume	175	175	175	175
Water	160	161.5	163	160
w/c	0.2	0.2	0.2	0.2*
w/b	0.16	0.17	0.17	0.16*
Silica sand – 1.6 mm	565	565	565	565
Silica sand – 0.5 mm	302	294.5	287	302
Silica flour	225	225	225	225
Dramix 65/35	40	40	40	40
Superplasticizer Sika 20 HE	30	30	30	30
Serenade Max		7.5	15	
SerBiotech				40

*Note: Water amount considered in water-cement and water-binder ratio evaluation includes the added water and the water in liquid bacteria (SerBiotech).

Each CC and HPC mixture were characterized by the slump test according to EN 12350-2, and each UHPC mixture by a slump flow test according to EN 12350-8. In accordance with EN 12390-3, the compressive strength of each mixture was determined at the age of 28 days using three 150 mm cubes per mixture.

3.2. Bacteria

Serenade® Max from BAYER is *Bacillus subtilis* encapsulated in Diatomaceous Earth, formulated as a wettable powder of natural origin containing 15.67% p/p (g/g) bacteria and bacterial content of 5.13×10^{10} CFU/g (colony forming units). Since bacteria are contained in a powder material, this product was incorporated in substitution of the sand of the smallest fraction (0/2 mm in CC and HPC and silica sand of maximum size 0.5 mm in the case of UHPC). Serenade® Max was added in the dosage of 7.5 kg/m³ in the mixes CC7.5DE HPC7.5DE and UHPC7.5DE and 15 kg/m³ in the mix named CC15DE HPC15DE and UHPC15DE. Due to the high DE absorption, to achieve a workable mix, extra water equal to 20% of the weight of the Serenade® Max content was added to compensate for the DE water absorption, as well as additional plasticizer content.

The liquid bacteria, SerBiotech solution, is a biodegradable, non-toxic, natural, and ecological liquid solution consisting of a combination of 66.3% *Bacillus* bacteria, 26.2% denitrifying bacteria, and 7.5% photosynthetic bacteria, containing in total 6.81×10^5 CFU/l bacteria. This type of liquid bacterial solution is commercially used in water treatment. Since bacteria is included in the liquid solution, this product was incorporated in substitution of the water content of the reference mix. Consequently, the water amount considered in the water-cement and water-binder ratio evaluation reported in Table 1 and Table 2 includes the added water and the amount of water in the liquid solution, which is

coherent with the w/c and w/b ratios of reference mixes. SerBiotech solution was added in substitution of 25% of the water content of the mix named CC25LB HPC25LB UHPC25LB. The mix with this solution was produced with the same plasticizer content as the reference mix since no effect on workability was detected by the addition of the agent.

3.3. Self-healing methodology

3.3.1. Specimen's geometry

To evaluate the self-healing capability of each mix, 8 cylinders of $\phi 100 \times 200$ mm per mix were prepared. After casting, the specimens were stored for 21 days in a humidity chamber at 20 °C and Relative Humidity of 95%; these cylinders were cut into $\phi 100 \times 50$ mm disks using a concrete circular saw. Each cylinder was cut into three disks, and two ends were discarded (Fig. 1 a and b). Some of these disks were pre-cracked and were used to evaluate self-healing capability using crack closure and water permeability. Chloride penetration tests were also performed on healed specimens to assess the protection provided by the healed crack against the penetration of chlorides. The methodologies followed are based on those proposed in the COST SARCOS Interlaboratory test groups, among which some studies have finished, but others are still ongoing [54,55].

To properly compare the relevant phenomena, additional uncracked disks housed in a humidity chamber at the same age as the primary samples were evaluated for chloride penetration.

The 21-day-old disks were pre-cracked using a splitting test to generate a residual crack width ranging from 50 to 450 μ m. The crack's width was measured the same day after pre-cracking and after 28 days of healing under various conditions. The objective of the wide range of crack widths was to have a variety of crack openings for each mixture

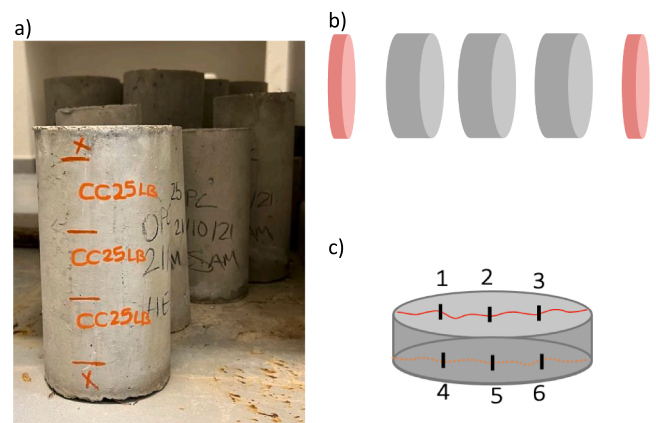


Fig. 1. A) cylinder marks before cutting the disks, b) cut of cylinders to obtain disks, c) crack measurement points after pre-cracking.

and condition to examine the trend of healing for a specific crack size range. Disks with larger crack openings than those within this range were discarded and excluded from this investigation. At least 6 specimens per mix and healing condition and four reference uncracked disks were evaluated for at least 22 specimens per mix.

3.3.2. Pre-cracking process and crack analysis

The splitting test setup was selected to pre-crack the disks of $\phi 100 \times 50$ mm. Samples are pre-cracked, targeting cracks near 500 μm during loading to obtain smaller residual crack size after unloading.

The disks' cracks were photographed with a YINAMA wireless optical microscope with 50-1000X magnification and a 2 MP camera. Crack width was measured in those photos, and a crack meter was used as a reference for the measurements. To obtain the representative value of crack width in each disk before and after healing, each surface of a disk was measured at three points located on the crack at intervals of 2.5 cm. These six values per disk were averaged to obtain the representative crack width of a disk (Fig. 1 c). In a few cases of having two (or multiple) cracks in a point, crack size is introduced as the summation of the two (or multiple) crack widths. Also, in the case of having a surface pore in the point, the crack size was measured at the nearest point disregarding the pore.

Crack Closing Ratio is the parameter used to evaluate the self-healing efficiency by means of crack closing in this study. The Crack Closing Ratio is calculated using the representative value of average crack width at six points in each disk before and after the healing period in the examined conditions, according to Eq.1.

$$\text{Crack Closing Ratio} = 1 - \frac{\text{Crack width after healing}}{\text{Crack width before healing}} \quad (1)$$

3.3.3. Low-pressure water permeability test

Fig. 2 depicts the setup used to determine water permeability. The same pre-cracked $\phi 100 \times 50$ mm disks used for the crack closing ratio analysis were sealed with resin (Sikaflex 11 FC) in the lateral surfaces to prevent water leakage through the lateral crack, and PVC tubes with an internal diameter of 100 mm and a height of 250 mm adhered to the disks with the same resin. A day after the disks were sealed, the bottom surface was wrapped with PVC tape to prevent water leakage before the test began. After preparing the water permeability setup, the tubes were filled with a 200 mm water column. After reading the initial water level, the bottom tape was removed to initiate the test (time 0). After removing the tape, the water head reduction was measured in minutes 0, 1, 5, 10, 15, 20, 25, and 30. The water flow (ml/30 min) in 30 min is determined by the total height loss in 30 min. Since the permeability test is conducted both before and after the healing time, the effect of healing on permeability was determined by calculating a Healing Ratio according to Eq. (2):

$$\text{Healing Ratio} = 1 - \frac{\text{Flow in 30min after healing}}{\text{Flow in 30min before healing}} \quad (2)$$

3.3.4. Chloride penetration test

A modified water penetration test proposed in previous studies [56,57] was performed by measuring the penetration of sodium chloride through the crack's path and the concrete surface by using its reaction with silver nitrate as a pigmentation method to detect the penetration.

This test was performed on the same disks and the same tubes used in the low-pressure water permeability test. The test was performed in the healed samples as well as in reference uncracked samples of each mix. Reference uncracked samples were cured in a humidity chamber at 20 °C and RH 95% until the test at the same age as the healed samples. A day after the water permeability test, the bottom cracked part of the pre-cracked samples was sealed using (Sikaflex 11 FC), to prevent leakage from the crack. A day after sealing the crack, samples were placed on the setup, and the tubes were filled with a 200 mm water column containing 33 g NaCl/liter, and the solution was kept inside tubes for 3 days. Afterward, the tubes and the resin parts were removed, and the samples were sawed perpendicular to the direction of the crack on the next day (Fig. 3 a). To prevent contamination produced by water cutting observed in a previous study [49], the sawing process was done by dry cutting. Subsequently, an AgNO_3 solution with a concentration of 0.1 mol/liter was sprayed on both surfaces of the cut disks, and disks were left for 24 h in an oven at 60–80 °C to improve the pigmented pattern profile. The concentration of 0.1 mol/liter has been recommended in earlier studies to have clearer white-dark boundaries [58–60].

On pigmented samples, two areas appear: the dark area presents the regions without penetration of the chloride, and the lighter area indicates the region containing chloride, which belongs to the area with risk for reinforcement corrosion [58,61,62]. The photos of the specimens after the reaction of AgNO_3 were taken with a Digital Camera.

An example of the pigmented disk (CC mix) is presented in Fig. 3b. The pattern shows two main regions of chloride penetration: the penetration through the crack (labeled as W) and the penetration through the matrix, starting from the surface in contact with the chloride solution (labeled as P_0). It is worth mentioning that in the uncracked reference samples, the measurement performed are only P_0 penetrations.

To quantify P_0 , four points were measured at intervals of 2 cm, starting with 1 cm spacing from the outer surface to avoid the gluing effect. The position of the points where the P_0 parameter is measured on both faces of a disk is indicated in Fig. 3. Similarly, three points are measured on each surface for the penetration produced along the crack pathway, maintaining a 2 cm distance from the surface to avoid the influence of matrix and crack penetration overlaps. In total, 8 values of P_0 and 6 values of W were used to obtain the representative value in each disk.

As shown in Fig. 3 bottom, in CC samples, P_0 was very clear to

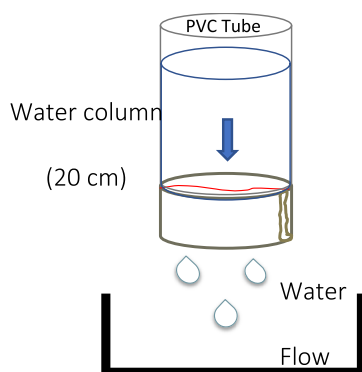


Fig. 2. Water permeability test setup, diagram, and photo of the setup.

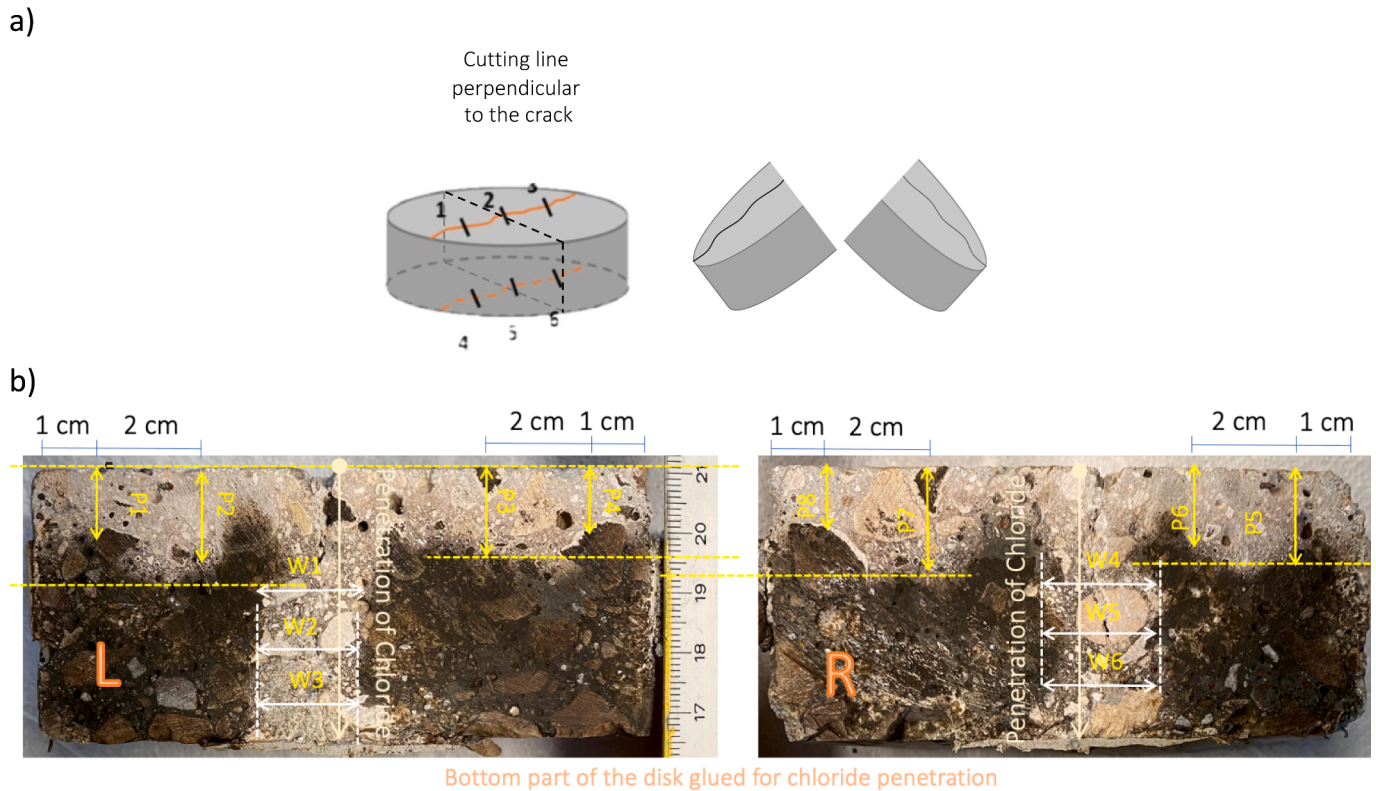


Fig. 3. A) diagram of the sawing plane of the pre-cracked disks and b) measurement points for the penetration of chlorides through the matrix and through the crack in the left (l) and right (r) half disks (this example refers to the cc mix).

measure, while for HPC and UHPC, P_0 was much smaller due to their low matrix porosity, coherent with the results obtained in previous studies [49]. In the case of the penetration through the crack, CC specimens have larger penetration if compared to UHPC samples.

3.4. Healing conditions

After pre-cracking the disks and performing the water permeability test before healing, specimens were divided into groups depending on their assigned healing condition to promote self-healing reactions. Three healing conditions were studied:

- 28 days immersion in water at 20 °C (labeled as WI),
- 28 days in a humidity chamber at 20 °C and relative humidity of 95% (labeled as HC), and
- 7 days in water immersion followed by 21 days in the humidity chamber (RH = 95%, 20 °C) (labeled as WH).

The objective of the WH condition was to evaluate whether the mixes with bacteria produced enough self-healing with only a reduced time under water immersion followed by a high humidity ambient that allows keeping the saturation level inside the matrix.

In addition, the uncracked reference disks of each mix were kept for 56 days in a humidity chamber until the testing time and were tested together with the pre-cracked and healed disks with the chloride penetration test. This way, these uncracked reference disks were the same age as the pre-cracked samples after healing.

During the healing process, the tubes glued on the disks for the permeability and penetration tests were kept glued on the disks until finishing the chloride penetration tests. To avoid cross-contamination between the series with different bacterial agents that healed in immersion conditions, the disks containing each type of bacteria healed in separate tanks.

4. Results and discussion

4.1. Characterization results

In terms of workability, the slump test results for CC and HPC mixes containing bacteria liquid solution were 7.5 and 2 cm, respectively, less than their respective reference mixes, which measured 20 and 8 cm. The effect of adding 7.5 and 15 kg/m³ of DE bacteria to CC mixes was compensated by adding more superplasticizer, and all series have a slump value of around 20 ± 4 cm (reference CC mix had 20 cm). Using a more effective superplasticizer into HPC mixtures containing DE bacteria provided for about the same workability as reference HPC mixtures (7 ± 1 cm). Adding 7.5 and 15 kg/m³ of DE bacteria to UHPC mixes results in 56 and 51 cm slump flows, compared to 61 cm for the reference mixtures. In contrast, liquid bacteria mixtures were more workable and behaved similarly to the UHPC reference mixtures with a 71 cm slump flow.

The compressive strength of each mix at 28 days is shown in Fig. 4. The CC mix obtained 41.50 MPa, which is greater than the CC15DE and CC25LB mixes, which produced 36.62 and 36.41 MPa, respectively. In addition, the CC7.5DE mixture had a higher compressive strength than the reference, which was 46.77 MPa.

All HPC mixtures including bacteria, showed a lower compressive strength than the reference mixture, which averaged 90.61 MPa. Compared to reference samples, HPC7.5DE and HPC15DE mixtures showed 4% and 9% reduced strength. Similarly, replacing 25% of the water with the bacterial solution resulted in a 27% lower strength than the reference mix.

In Ultra High-Performance mixes, UHPC7.5DE has about the same strength as the reference UHPC mix. In contrast, the compressive strength of UHPC15DE mix decreased by 7%, compared to the reference UHPC mix.

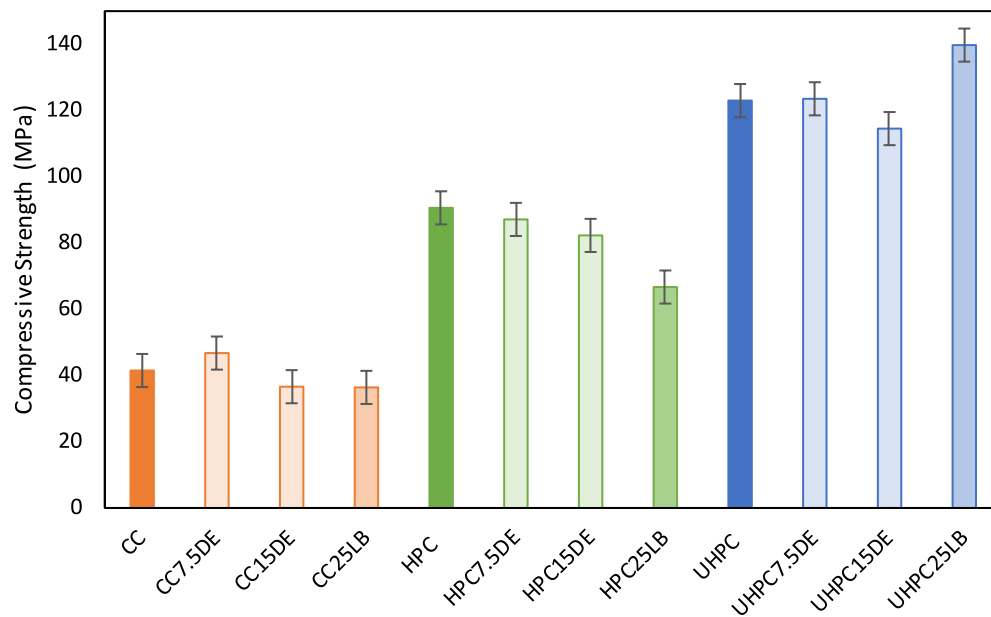


Fig. 4. Compressive strength of mixes at 28 days (average and standard deviation).

4.2. Crack closing

The self-healing capability in terms of visual crack closing, evaluated with the Crack Closing ratio in Eq (1), is presented in Fig. 5 (left column) for the three concrete types. In addition, a trendline for each healing condition has been included in these graphs to make the analysis easier. The trendlines depicted have been obtained following this procedure: a) the linear trendline of a mix and healing condition was obtained (e.g., CC healed in WI, CC healed in WH and CC healed in HC), b) the representative trendline slope of each mix was obtained by averaging the slopes for the three healing conditions in the same mix, and finally, c) the represented fitting line for each mix and healing condition was obtained forcing the same slope (minimizing least squares difference) and keeping as a free parameter the vertical intercept of the line. In this way, the efficiency depending on the mix and healing condition, can be visually interpreted. This analysis was made regardless of the presence or absence of bacteria.

Fig. 5 depicts the crack closing ratio of concrete mixes separated depending on their healing conditions. Most of the CC specimens healed in WI condition with cracks lower than 200 μm had significant crack closure with values around 80% to 100%. Specimens healed in WH condition with almost complete crack closure had initial cracks between 100 and 120 μm . The rest of the specimens healed in WH condition had crack closure values, decreasing from 90% to 40% as the initial crack width increased. Specimens stored in HC had crack closure values between 0% and 60%, generally lower than 50%.

HPC mixes with bacteria HPC7.5DE, HPC15DE, and HPC25LB healing in WI had nearly complete crack closure for initial cracks below 150 μm , with higher values than the reference HPC mix. For cracks larger than 150 μm , the crack closure ratios decrease more abruptly than in CC mixes. On the contrary, specimens healed in HC had crack closure values lower than 20% regardless of using bacteria. This shows the inability of only high humidity conditions to activate the healing reactions, which is coherent with other results in the literature [15].

Specimens from UHPC mixes healed in WI also showed better crack closing compared to WH and HC conditions, both in mixes with and without bacteria, with more than 60% healing for the samples with initial crack up to 150 μm . In UHPC mixes, the closing ratio healing in HC was mostly below 20%.

The type of mix (CC, HPC, or UHPC) and the curing condition (WI, WH, or HC) are more relevant for the crack closing ratio than the healing agent used, and no clear improvements on this parameter were detected

due to the presence of the bacteria of this work. The presence of water was critical for the healing reactions in all concretes, both for reference mixes and all mixes with bacteria. Additionally, CC and HPC healing in WH conditions had a closing ratio usually higher than 60%, more similar to specimens healed in WI conditions than those healed in HC, which shows that only 7 days of water immersion can provide values of crack closing that are comparable to one month of water immersion. In addition, CC mixes exhibited greater crack closing values than HPC mixes, whereas UHPC mixes had the lowest values. This result is clearly seen in the average trendlines in Fig. 5. This fact could be related to the crack's lower tortuous surface for HPC and UHPC than for CC due to their higher strength.

The low water-binder ratio in HPC and UHPC improves the bond between hardened cement paste and aggregate, which makes more likely a transgranular fracture mode (crack path travels through the aggregate) instead of the fracture mode of the crack path developing around the coarse aggregate [63,64]. The fracture mode with the crack path developing around the aggregates results in a more tortuous fracture path [63]. Crack tortuosity is related to lower transport properties [65]; however, it has also been related to increased chloride penetration for cracks between 150 and 370 μm [66], with less effect as crack width increases [65,66]. Crack tortuosity is also affected by the presence of fibers and the bond between fibers and matrix [65,67], and by the accumulation of healing products in the crack, which increases surface roughness, and, therefore, changes crack geometry [65].

4.3. Self-healing in water permeability

The results of the Healing ratio (Eq.2) analyzed by means of the water permeability test are presented in the right column of Fig. 5. A common trendline was determined with the same criteria explained in section 3.2 to allow visual analysis of the results.

The analysis confirms the interpretation is done for cracks closing, with a clear influence of healing condition, a big variability of the results, and a reduction of the healing efficiency when crack width increases.

CC specimens containing bacteria healed in WI had healing ratios between 60 and 100% when initial crack widths were below 300 μm , higher than reference samples healed in the same condition. The CC samples healed in WH condition and had healing ratios higher than 80% for cracks until 250 μm . HPC specimens with bacteria showed an

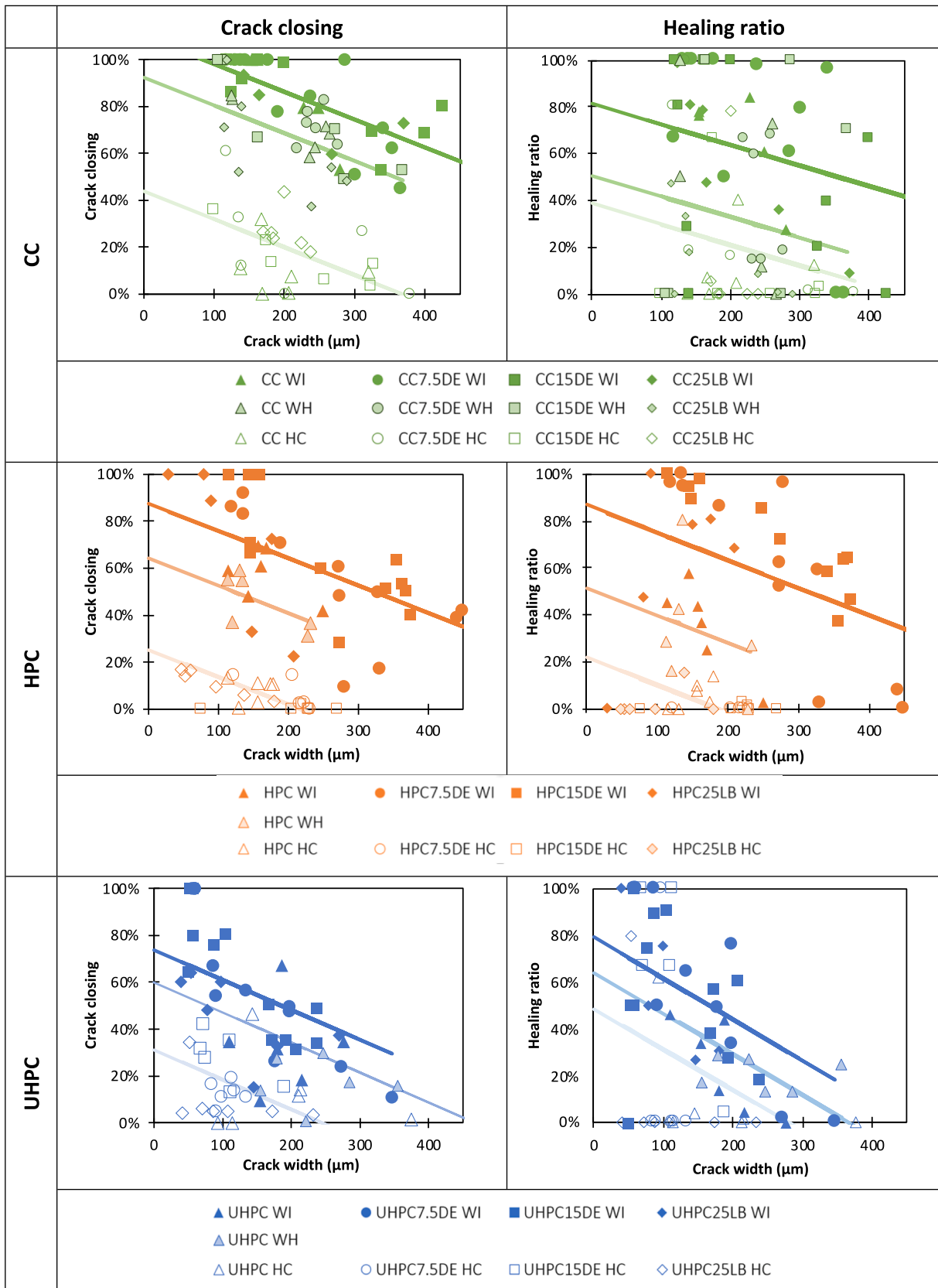


Fig. 5. Closing ratio (left column) and healing ratio (right column) of the mixes of this study depending on initial crack width.

improvement in the healing ratio, with values over 50% until 400 μm of initial crack width when healing in WI. UHPC specimens healed in WI with initial crack widths below 100 μm had practically complete healing, which is reduced progressively to a healing ratio of 0% for 300 μm cracks.

Similarly, the crack closing results show that the mix type and curing condition are more relevant for the healing ratio than the healing agent used. Also, CC, HPC, and UHPC specimens healing in HC generally had healing ratios below 20%, except for some specimens containing bacteria with crack width smaller than 200 μm .

4.4. Crack closing ratio vs. Healing ratio

Many studies only analyze crack closure, though the information on how a crack heals in terms of water permeability changes provides information more relevant to the durability of a structure. Therefore, the comparison of crack closure and healing ratios is of interest. Fig. 6 depicts these two parameters for the specimens tested in this work after 28-day healing in different conditions.

Regarding specimens healed in HC, CC specimens had crack closure values in the 0–50% range, but healing ratios were generally below 20%. In HPC specimens, crack closure and healing ratios were similar. However, in UHPC specimens, several specimens had high values of healing ratios with low crack closing ratios. This indicates potentially different healing mechanisms in the three concrete types. Regarding specimens healed in WI and WH, most HPC and UHPC specimens are also more likely to be close to the diagonal line (similar crack closing and healing ratios), which is coherent with other study [12], which reported a direct relation between crack closure and healing ratio in the case of healing in water immersion. Other study [68] reported crack closing efficiency of 100% for cracks of 0.3 and 0.4 mm, incorporating a self-healing agent with *Bacillus cohnii* and healing in water immersion condition, with 82–91% healing ratios for the water permeability test.

The trendlines presented in Fig. 6 were generated using only points with ratios other than “1” or “0” to study only those influencing this property. In all the cases, the points are gathered in broad lines steeper than the diagonal and the position of the trend line changes depending on the matrix, moving from right to left when changing from CC to HPC and UHPC. This means that CC mixes are more likely to have high values of crack closing ratios that do not correspond with a high value in the healing ratio measured by means of the permeability test. On the other hand, UHPC mixes are more likely to have high values of healing ratio that do not correspond with a visual crack closing of the crack. Another interpretation is that, to have an efficient self-healing effect in the permeability test, a crack closing ratio higher than 50% is required in UHPC if compared CC.

4.5. Self-healing through chloride penetration

4.5.1. Penetration through the crack

Fig. 7 shows the values of chlorides' penetration through the cracks walls (W) and the trendlines obtained with the same criteria as in previous sections. The results show higher penetration for healed CC specimens than HPC, and the lowest penetration values were obtained in UHPC mixes. The average values of W obtained in each group are also collected in Table 3.

In CC mixes, specimens healed in HC had much larger penetration than specimens healed in WH or WI. However, the penetration values in HPC and UHPC specimens are more similar in specimens that healed in HC, WH or WI conditions. UHPC specimens, with and without bacteria, had the lowest penetration if compared with other concrete types, with nearly the same horizontal trendline (which indicates that there is no relation between the W value measured and the initial crack width), regardless of healing condition and regardless of the addition of bacteria. This indicates a noteworthy intrinsic capability of UHPC in maintaining low chloride penetration for cracks up to 400 μm . On the

contrary, in CC mixes, the trendlines had a higher inclination, indicating a dependence on the initial crack width (larger penetration W values with larger cracks). As expected, HPC mixes show intermediate behavior between CC and UHPC, and this penetration does not surpass 10 mm.

Regarding the effects of adding bacteria, CC specimens with bacteria had a lower penetration W through the crack compared to CC reference mixes healed in the same condition. CC specimens with liquid bacteria (CC25LB) healed in WI showed very high protection against the penetration of chlorides for cracks up to 350 μm . HPC specimens with bacteria healed in WI could maintain almost complete protection against chloride for cracks lower than 250 μm .

4.5.2. Penetration through the matrix

The average values of chloride penetration through the matrix P_0 for each group are collected in Table 3. As a reference, the average values obtained in uncracked specimens is also included as Ref P_0 .

In CC mixes, the highest penetration through the matrix in uncracked reference specimens was obtained in CC15DE mix, with an average value of 21.19 mm, followed by CC with 12.8 mm, CC7.5DE with 7.75 mm, and CC25LB with 6.38 mm. Because of the dense matrix of HPC, all HPC mixes showed average matrix penetration values <2 mm in uncracked specimens, consistent with earlier research [49]. In uncracked specimens, UHPC mixes without bacteria had a matrix penetration of less than 3 mm, whereas UHPC mixes with bacteria had a matrix penetration of less than 2 mm.

Similar to prior research findings [45], almost all CC mixes with bacteria that were cracked and healed in WI and WH conditions had negligible matrix penetration, confirming the effect of bacteria on lowering porosity. As expected, specimens healed in HC had P_0 values like the reference of uncracked specimens (Ref P_0). Research on self-healing already reported the substantial effect of water in healing [41,57], and Escoffres et al. [69] proposed that specimens healed in a humidity chamber can be used as references since in practice, HC do not promote healing. Healed HPC specimens had a penetration below 2 mm in all mixes, as in the uncracked specimens. In UHPC healed specimens, regardless of healing condition and the presence of bacteria, the values of P_0 were below 4 mm, with lower values (below 1 mm) in mix that contained bacteria in DE, which shows the capability of these agents on reducing porosity.

4.6. Discussion on the efficiency of the self-healing agents

In previous sections it was assumed that the inclination of the trendline is representative of the type of concrete mix. This section will evaluate the efficiency of the self-healing agents with the same criteria. With this procedure, the value of intercept with the vertical axis can be obtained separately for each concrete mix, healing condition and self-healing agent. This value represents whether a trendline is higher or lower in the graph and, therefore, shows better or worse healing efficiency in the parameter that is being analyzed (crack closing ratio, healing ratio or chloride penetration parameters). This value is displayed in Table 4, where the improvements larger than 5% have been indicated with a green upwards arrow, worsening larger than 5% with an orange downward arrow, and similar results with an almost equal symbol.

Analyzing the parameters of crack closing, healing ratio, and chloride penetration through the crack, when the specimens of either mix (CC, HPC and UHPC) healed in WI conditions, there was a benefit from the presence of bacteria, regardless of the agent. Most of the mixes with bacteria showed an improvement regarding the penetration of chlorides (W), to the exception of the group CC healing in HC conditions. These improvements were especially noticeable in the CC group healing in WI conditions. When healing in HC conditions, this benefit could only be detected in crack closing and healing ratios in the CC mix, while HPC and UHPC had dispersed results.

The bacterial agent immobilized in DE was used in two dosages, 7.5

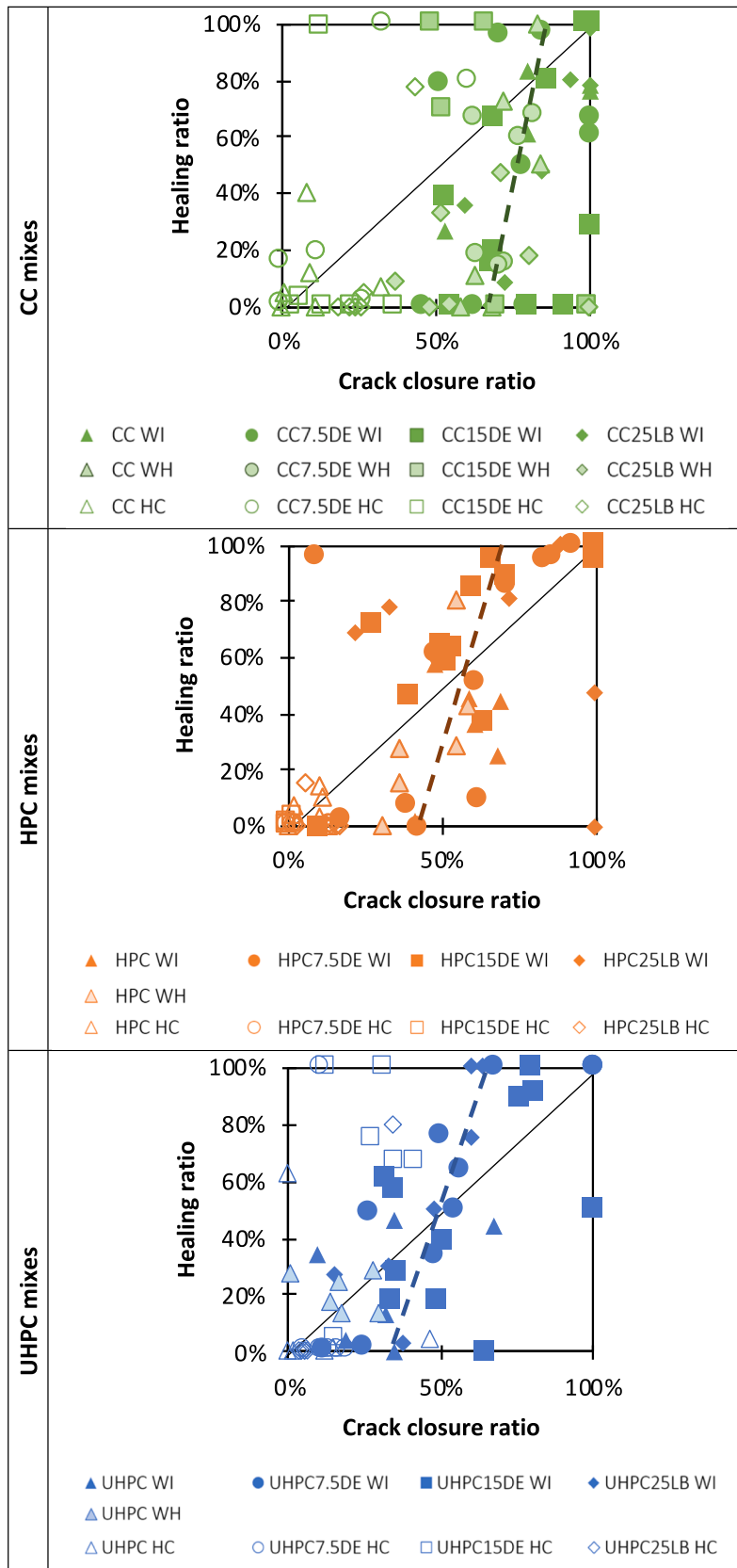


Fig. 6. Crack closure ratio vs Healing ratio by means of water permeability test, CC (top), HPC (middle), and UHPC (bottom).

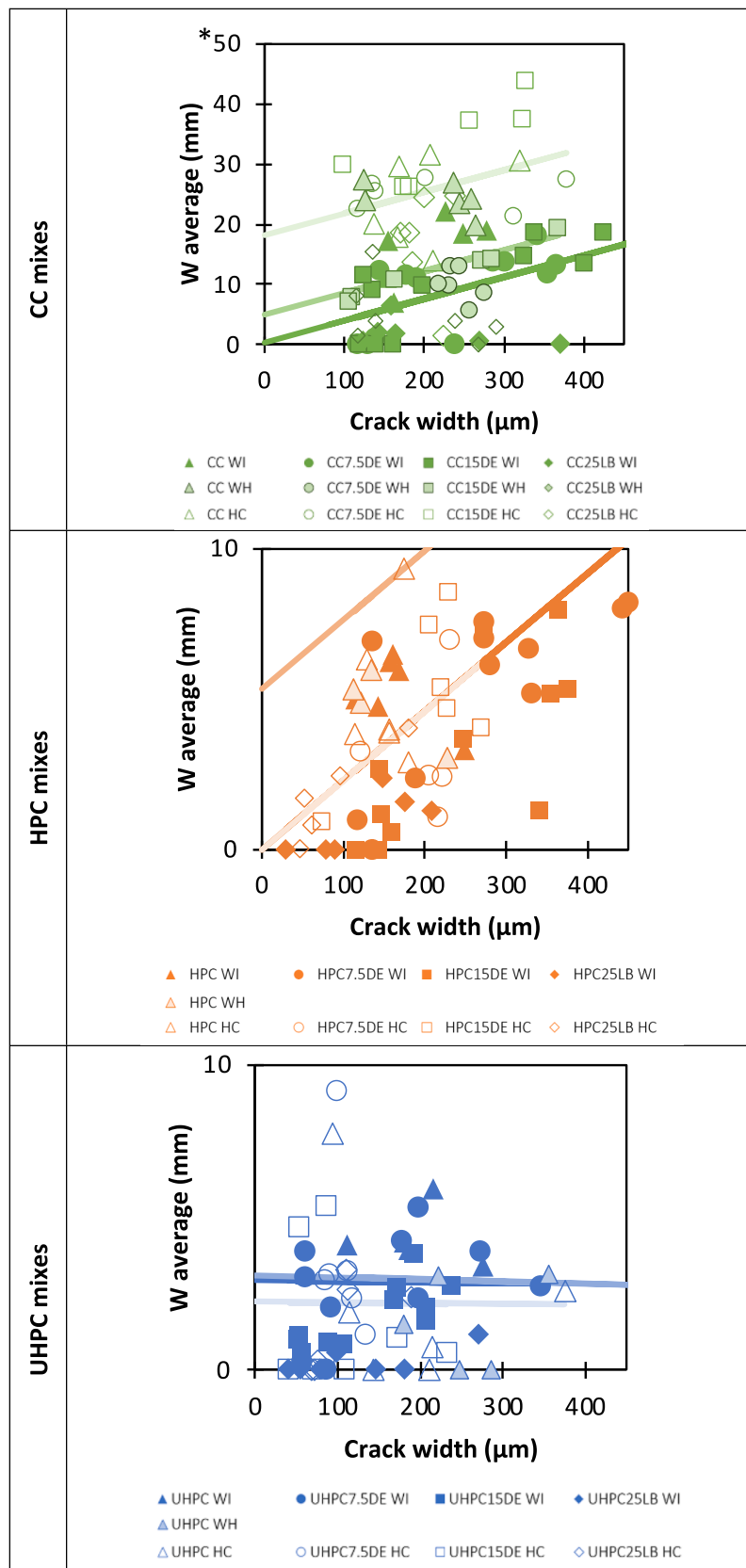


Fig. 7. Chloride penetration along the crack (W) after healing depending on the type of mix (CC, HPC, UHPC), their initial crack width and their healing condition. *Note: The scale of the vertical axis for CC varies from that of HPC and UHPC due to the high chloride penetration value of CC.

Table 3

Values of penetration through the matrix in uncracked specimens (Ref P₀), average crack width before and after healing, and penetration P₀ and W values in all the groups studied.

	CC				HPC			UHPC				
	CC	CC 7.5DE	CC 15DE	CC 25LB	HPC	HPC 7.5DE	HPC 15DE	HPC 25LB	UHPC	UHPC 7.5DE	UHPC 15DE	UHPC 25LB
Ref P ₀ (mm)	12.79	7.75	21.19	7.13	1.58	1.88	1.29	0.00	2.92	1.44	0.15	1.77
Avg crack bef. (μm)	205	238	248	196	159	258	255	108	206	129	136	116
Avg crack after (μm)	96	90	104	88	100	157	159	70	170	74	89	88
WI												
P ₀ (mm)	0.08	1.51	1.14	0.09	0.00	0.55	0.46	1.28	3.92	0.64	0.35	2.63
W (mm)	15.80	9.18	10.37	1.91	5.28	5.40	4.43	0.87	6.85	3.45	1.72	0.25
WH												
P ₀ (mm)	4.34	0.64	0.67	0.50	0.00	–	–	–	3.05	–	–	–
W (mm)	24.26	9.96	12.15	5.30	9.00	–	–	–	3.52	–	–	–
HC												
P ₀ (mm)	12.79	7.81	19.35	9.71	0.00	0.88	1.02	0.54	2.48	2.41	0.82	3.26
W (mm)	23.87	25.11	33.36	20.80	5.03	3.21	5.16	0.54	2.15	3.64	1.42	1.66

Table 4

Values of the vertical intercept of the trendlines with the vertical axis. ↑ indicates > 5% benefit in that parameter, ↓ a worsening > 5%, and ≈ indicates similar results.

Crack Closure Ratio											
Healing Exposure		WI			HC			WH			
Concrete		CC	HPC	UHPC	CC	HPC	UHPC	CC	HPC	UHPC	
Healing Agent	Ref	1.10	0.77	0.57	0.34	0.26	0.37	0.96	0.71	0.48	
	7,5DE	1.12≈	0.88↑	0.77↑	0.47↑	0.30↑	0.27↓	1.01≈			
	15DE	1.14≈	0.94↑	0.79↑	0.43↑	0.24↓	0.41↑	0.99≈			
	25LB	1.13≈	0.84↑	0.61↑	0.50↑	0.22↓	0.23↓	0.81↓			
Healing Ratio											
Healing Exposure		WI			HC			WH			
Concrete		CC	HPC	UHPC	CC	HPC	UHPC	CC	HPC	UHPC	
Healing Agent	Ref	0.89	0.54	0.56	0.28	0.24	0.45	0.57	0.67	0.63	
	7,5DE	0.87≈	0.89↑	0.88↑	0.55↑	0.23≈	0.35↓	0.62↑			
	15DE	0.70↓	1.02↑	0.74↑	0.37↑	0.25≈	0.87↑	0.64↑			
	25LB	0.72↓	0.77↑	0.77↑	0.31↑	0.14↓	0.30↓	0.35↓			
Chloride penetration (W)											
Healing Exposure		WI			HC			WH			
Concrete		CC	HPC	UHPC	CC	HPC	UHPC	CC	HPC	UHPC	
Healing Agent	Ref	8.40	1.48	6.89	14.07	1.55	2.20	16.67	4.30	3.57	
	7,5DE	0.18↑	0.00↑	3.49↑	17.36↓	0.00↑	3.66↓	1.14↑			
	15DE	0.42↑	0.00↑	1.76↑	25.13↓	0.47↑	1.44↑	4.27↑			
	25LB	0.00↑	0.00↑	0.63↑	13.55≈	0.00↑	1.68↑	0.00↑			

and 15 kg/m³. The addition of 15 kg/m³ of this agent seems to produce no benefits and decreased compression strength by 25%, 5 %, and 7% in CC, HPC, and UHPC mixes. Moreover, in CC and HPC mixes, it led to an increase in the setting time, and this mix showed no benefits regarding the penetrability of the matrix than the reference and CC7.5DE. These results were also reported in other research [28]; where excessive amounts of mineral precursors had a negative effect on concrete properties, setting time, and final strength.

In previous studies [25,44,70], it has been demonstrated that the healing reactions observed in bacteria concrete are attributed to metabolic activity. The negatively charged cell wall of bacteria attracts Ca²⁺ ions from the cement matrix. These Ca²⁺ ions then react with CO₃²⁻ ions to form calcium carbonate precipitates around the bacterial cells. The survival and activation of bacteria in concrete are essential for effective healing. The concrete matrix, with its dense structure and high pH (around 12–13) in uncracked conditions, presents challenging conditions for the bacteria [71].

A study on normal-strength concrete [25] found that autoclaved and active bacteria could fill cracks and reduce water permeability to a similar extent as autogenous healing in reference specimens. This suggests that autogenous healing is more significant in these properties than bacterial activity. This observation aligns with the present study's findings in normal-strength concrete, where no crack closure or water

permeability improvements were observed when using bacterial agents. However, in this work, incorporating bacterial agents improved healing performance, particularly in high-performance concrete (HPC) and ultra-high-performance concrete (UHPC), with a more pronounced enhancement in protection against chloride penetration.

The enhanced response observed when using bacteria in the study of chloride penetration may be attributed to a decrease in surface pH due to the carbonation [72]. This phenomenon occurs especially when the samples are exposed to a chloride-rich environment, leading to pH values of 8–9 [73]. In this study, products containing *Bacillus subtilis* and *Bacillus sphaericus* were employed. Certain strains of *Bacillus sphaericus* have been reported to exhibit growth and germination in a wide range of alkaline pH conditions, with an optimal pH range of 7–9 and slow (but active) growth at pH levels of 10–11 [74]. Similarly, certain strains of *Bacillus subtilis* have demonstrated survivability at high pH levels [73]. However, further research is required to confirm this hypothesis.

Various healing agents, such as supplementary cementitious materials (SCMs), including silica fume, slag, fly ash, and crystalline admixtures, have been introduced into UHPC to assess their potential for enhancing the healing process [70]. However, limited investigations have been conducted on the use of bacteria in UHPC. The potential of bacterial treatment in UHPC is suggested by another study [75], which focused on treating the steel fibers of UHPC with *Sporosarcina pasteurii*.

The results indicated that such treatment increased the precipitation of calcium carbonate crystals on the fiber surfaces, resulting in enhanced surface roughness and hydrophilicity, ultimately improving mechanical performance.

4.7. Discussion on the penetration of chlorides in cracks

The ratio between the chloride penetration through the crack (W) and the penetration through the matrix (P_0) in CC and UHPC specimens healed in HC are very similar and near to 2 ± 1 , which means that conditions where healing is not promoted (HC), the penetration through the cracks, is approximately two times the penetration through the matrix. In the case of conditions that promote healing, such as the presence of a healing agent or an adequate healing condition (WI or WH), this ratio is clearly higher due to a small value of the matrix penetration (P_0), because of the densification of the matrix and potentially of the healing reactions on the surface. Reduction of matrix penetration has also been reported in the study [73], in which the concrete surface has lower pH due to carbonation, while the inner matrix has high pH and a drier environment, which is too harsh for the bacteria growth and, thus, the healing rate drops noticeably along the pathway of the crack.

In addition, a poor or broad interfacial transition zone (ITZ) between cement paste and aggregates is known to allow the penetration of the chlorides [37], while the decrease in ITZ makes the cementitious material have a denser matrix [42]. In this study, a higher penetration circling aggregate was observed in samples of conventional and high-performance concrete specimens, leading to higher penetration values through cracks (example in Fig. 8).

The silver nitrate colorimetric method is a very simple and quick way to measure the chloride penetration depth in concrete. The brown area is assumed to be a chloride-free area; however, it is not really chloride-free [76]. The chloride content at the color change boundary has been reported to be between 0.01% and 1.41% by the mass of the cement [62,77]. The heterogeneity of concrete and the different methods used for obtaining the chloride concentration and for obtaining the powder for the analysis are considered responsible for this variation [76], as well as parameters such as mix composition or internal and environmental conditions [78].

Despite the fact that the colorimetric method does not correlate exactly with other methods for obtaining chloride concentration, it is a quick preliminary estimation of the chloride penetration depth. The concentration used in this study of 0.1 mol/l is the most appropriate for reducing difficult to detect coloring profiles reducing the problems mentioned [77], and it can detect even a small amount of 0.01% free chloride content by the mass of cement [61]. In addition, the chloride concentration at the chloride penetration depth detected by the spray test roughly corresponds to the commonly accepted value for the critical chloride concentration [78]. Therefore, the white area detected on a freshly split concrete surface can be considered an area at risk for steel reinforcement corrosion [62]. This information is useful for further analysis of the chloride profile with more accurate methods.

5. Conclusions

The effect of some commercial bacterial products on the self-healing capability of more than 300 specimens of CC, HPC, or UHPC is evaluated by performing 3 tests (crack closing, water permeability, and chloride permeability). From the obtained results, the following conclusions can be drawn:

1. Regarding visual closure of the cracks, the incorporation of the bacteria showed improvements in the crack closing ratio higher than 5% in HPC and UHPC healing in WI conditions and in CC healing in HC conditions. One week of water immersion significantly improved



Fig. 8. Effect of ITZ on chloride penetration of conventional concrete specimen.

- the crack closure capability compared to specimens healed in a humidity chamber.
2. Regarding the improvements in water tightness, the healing ratio of specimens healed in water immersion conditions is higher than in other conditions; however, these ratios are inferior to those obtained in crack closure.
3. Conventional concrete mixes are more likely to have high values of visual healing of the crack that do not correspond with a recovery of the water tightness. On the contrary, HPC and UHPC mixes are more likely to have high values of recovery of water tightness that do not correspond with a visual crack closing of the crack. For UHPC to have an effective self-healing effect in the permeability test, it must have a crack closing ratio higher than 50%.
4. Due to the dense matrix of high-performance and ultra-high-performance concrete specimens, their natural resistance to chloride penetration for cracks up to 400 μm is quite low, less than 10 mm, and bacterial addition has no discernible effect. In contrast, the chloride penetration reduction of conventional concrete specimens containing bacteria was much greater than that of specimens containing no bacteria. CC specimens containing liquid bacteria (CC25LB) and cured in WI showed improved chloride penetration resistance for cracks up to 350 μm .
5. The ratio of chloride penetration through the crack to chloride penetration through the matrix (W/P_0) in CC and UHPC specimens cured in HC are very similar and near 2.

CRediT authorship contribution statement

Hesam Doostkami: Writing – review & editing, Writing – original draft, Investigation, Conceptualization. **Javier de Jesús Estacio Cumberbatch:** Investigation. **Sidiclei Formagini:** Investigation, Conceptualization. **Pedro Serna:** Writing – review & editing, Validation, Supervision, Resources, Methodology, Conceptualization. **Marta Roig-Flores:** Writing – review & editing, Validation, Supervision, Methodology.

Declaration of Competing Interest

The authors declare that they have no known competing financial interests or personal relationships that could have appeared to influence the work reported in this paper.

Data availability

No data was used for the research described in the article.

Acknowledgments

The authors thank Sika and Serbiotec for supplying different materials used in the experimental campaign.

References

- [1] H.M. Jonkers, E. Schlangen, Self-healing of cracked concrete: A bacterial approach, *Proc. 6th Int. Conf. Fract. Mech. Concr. Struct.* 3 (2007) 1821–1826.
- [2] N. De Belie, E. Gruyaert, A. Al-Tabbaa, P. Antonaci, C. Baera, D. Bajare, A. Darquennes, R. Davies, L. Ferrara, T. Jefferson, C. Litina, B. Miljevic, A. Otlewska, J. Ranogajec, M. Roig-Flores, K. Paine, P. Lukowski, P. Serna, J. M. Tulliani, S. Vucetic, J. Wang, H.M. Jonkers, A review of self-healing concrete for damage management of structures, *Adv. Mater. Interfaces* 5 (2018) 1–28, <https://doi.org/10.1002/admi.201800074>.
- [3] EN 1992-1-1, Eurocode 2: design of concrete structures – Part 1–1: general rules and rules for buildings (+AC: 2008) (+AC: 2010), Brussels, (2005).
- [4] British Standards Institution BSI, Structural use of concrete — Part 1: Code of practice for design and construction - BS 8110-1: 1997, Br. Stand. (1973).
- [5] C. Edvardsen, Water permeability and autogenous healing of cracks in concrete, *ACI Mater. J.* 96 (1999) 448–454, <https://doi.org/10.14359/645>.
- [6] S. Granger, A. Loukili, G. Pijaudier-Cabot, G. Chanvillard, Experimental characterization of the self-healing of cracks in an ultra high performance cementitious material: Mechanical tests and acoustic emission analysis, *Cem. Concr. Res.* 37 (2007) 519–527, <https://doi.org/10.1016/j.cemconres.2006.12.005>.
- [7] H.W. Reinhardt, M. Jooss, Permeability and self-healing of cracked concrete as a function of temperature and crack width, *Cem. Concr. Res.* 33 (2003) 981–985, [https://doi.org/10.1016/S0008-8846\(02\)01099-2](https://doi.org/10.1016/S0008-8846(02)01099-2).
- [8] S. Granger, A. Loukili, G. Pijaudier-Cabot, G. Chanvillard, Mechanical characterization of the self-healing effect of cracks in Ultra High Performance Concrete (UHPC), in: *Proc. Third Int. Conf. Constr. Mater. Performance, Innov. Struct. Implic. ConMat*, 2005: pp. 22–24.
- [9] L. Ferrara, E.C. Asensio, F. Lo Monte, M.R. Flores, M.S. Moreno, D. Snoeck, T. Van Mullem, N. De Belie, Experimental Characterization of the Self-Healing Capacity of Cement Based Materials: An Overview, (2018) 454. <https://doi.org/10.3390/icem18-05322>.
- [10] M. Davolio, S. Al-Oubaidi, M.Y. Altomare, F. Lo Monte, L. Ferrara, A methodology to assess the evolution of mechanical performance of UHPC as affected by autogenous healing under sustained loadings and aggressive exposure conditions, *Cem. Concr. Compos.* 139 (2023), 105058, <https://doi.org/10.1016/j.cemconcomp.2023.105058>.
- [11] E. Cuenca, V. Postolachi, L. Ferrara, Cellulose nanofibers to improve the mechanical and durability performance of self-healing Ultra-High Performance Concretes exposed to aggressive waters, *Constr. Build. Mater.* 374 (2023), 130785, <https://doi.org/10.1016/j.conbuildmat.2023.130785>.
- [12] M. Roig-Flores, F. Pirritano, P. Serna, L. Ferrara, Effect of crystalline admixtures on the self-healing capability of early-age concrete studied by means of permeability and crack closing tests, *Constr. Build. Mater.* 114 (2016) 447–457, <https://doi.org/10.1016/j.conbuildmat.2016.03.196>.
- [13] A. Beglarigale, D. Eyice, B. Tutkun, H. Yazici, Evaluation of enhanced autogenous self-healing ability of UHPC mixtures, *Constr. Build. Mater.* 280 (2021), 122524, <https://doi.org/10.1016/j.conbuildmat.2021.122524>.
- [14] J.Y. Guo, J.Y. Wang, K. Wu, Effects of self-healing on tensile behavior and air permeability of high strain hardening UHPC, *Constr. Build. Mater.* 204 (2019) 342–356, <https://doi.org/10.1016/j.conbuildmat.2019.01.193>.
- [15] M. Roig-Flores, S. Moscato, P. Serna, L. Ferrara, Self-healing capability of concrete with crystalline admixtures in different environments, *Constr. Build. Mater.* 86 (2015) 1–11, <https://doi.org/10.1016/j.conbuildmat.2015.03.091>.
- [16] D. Snoeck, N. De Belie, Repeated Autogenous Healing In Strain-Hardening Cementitious Composites By Using Superabsorbent Polymers, *J. Mater. Civ. Eng.* 28 (2016) 04015086, [https://doi.org/10.1061/\(asce\)mt.1943-5533.0001360](https://doi.org/10.1061/(asce)mt.1943-5533.0001360).
- [17] J. Wang, K. Van Tittelboom, N. De Belie, W. Verstraete, Use of silica gel or polyurethane immobilized bacteria for self-healing concrete, *Constr. Build. Mater.* 26 (2012) 532–540, <https://doi.org/10.1016/j.conbuildmat.2011.06.054>.
- [18] A. Gross, D. Kaplan, K. Baker, Removal of chemical and microbiological contaminants from domestic greywater using a recycled vertical flow bioreactor (RVFB), *Ecol. Eng.* 31 (2007) 107–114, <https://doi.org/10.1016/j.ecoleng.2007.06.006>.
- [19] S. Chaturvedi, R. Chandra, V. Rai, Isolation and characterization of *Phragmites australis* (L.) rhizosphere bacteria from contaminated site for bioremediation of colored distillery effluent, *Ecol. Eng.* 27 (2006) 202–207, <https://doi.org/10.1016/j.ecoleng.2006.02.008>.
- [20] J.Y. Wang, D. Snoeck, S. Van Vlierberghe, W. Verstraete, N. De Belie, Application of hydrogel encapsulated carbonate precipitating bacteria for approaching a realistic self-healing in concrete, *Constr. Build. Mater.* 68 (2014) 110–119, <https://doi.org/10.1016/j.conbuildmat.2014.06.018>.
- [21] Q. Chunxiang, W. Jianyun, W. Ruixing, C. Liang, Corrosion protection of cement-based building materials by surface deposition of CaCO₃ by *Bacillus pasteurii*, *Mater. Sci. Eng. C* 29 (2009) 1273–1280, <https://doi.org/10.1016/j.msec.2008.10.025>.
- [22] W. De Muynck, D. Debrouwer, N. De Belie, W. Verstraete, Bacterial carbonate precipitation improves the durability of cementitious materials, *Cem. Concr. Res.* 38 (2008) 1005–1014, <https://doi.org/10.1016/j.cemconres.2008.03.005>.
- [23] J. Wang, Y.C. Ersan, N. Boon, N. De Belie, Application of microorganisms in concrete: a promising sustainable strategy to improve concrete durability, *Appl. Microbiol. Biotechnol.* 100 (2016) 2993–3007, <https://doi.org/10.1007/s00253-016-7370-6>.
- [24] P. Ghosh, S. Mandal, B.D. Chattopadhyay, S. Pal, Use of microorganism to improve the strength of cement mortar, *Cem. Concr. Res.* 35 (2005) 1980–1983, <https://doi.org/10.1016/j.cemconres.2005.03.005>.
- [25] K. Van Tittelboom, N. De Belie, W. De Muynck, W. Verstraete, Use of bacteria to repair cracks in concrete, *Cem. Concr. Res.* 40 (2010) 157–166, <https://doi.org/10.1016/j.cemconres.2009.08.025>.
- [26] L. Li, Q. Zheng, Z. Li, A. Ashour, B. Han, Bacterial technology-enabled cementitious composites: A review, *Compos. Struct.* 225 (2019), 111170, <https://doi.org/10.1016/j.compstruct.2019.111170>.
- [27] Y.Ç. Erşan, F.B. Da Silva, N. Boon, W. Verstraete, N. De Belie, Screening of bacteria and concrete compatible protection materials, *Constr. Build. Mater.* 88 (2015) 196–203, <https://doi.org/10.1016/j.conbuildmat.2015.04.027>.
- [28] H.M. Jonkers, A. Thijssen, G. Muys, O. Copuroglu, E. Schlangen, Application of bacteria as self-healing agent for the development of sustainable concrete, *Ecol. Eng.* 36 (2010) 230–235, <https://doi.org/10.1016/j.ecoleng.2008.12.036>.
- [29] H.M. Jonkers, A. Thijssen, Bacteria Mediated of Concrete Structures, 2nd Int. Symp. Serv. Life Des. Infrastruct. 4-6 Oct. 2010, Delft, Netherlands. (2010) 833–840.
- [30] H.M. Jonkers, Bacteria-based self-healing concrete, *Heron.* 56 (1–2) (2011) 5–16.
- [31] J.Y. Wang, N. De Belie, W. Verstraete, Diatomaceous earth as a protective vehicle for bacteria applied for self-healing concrete, *J. Ind. Microbiol. Biotechnol.* 39 (2012) 567–577, <https://doi.org/10.1007/s10295-011-1037-1>.
- [32] S.C. Hunt, Method and system for bioremediation of contaminated soil using inoculated diatomaceous earth, US Patent 5570973, (1996).
- [33] R. Nanayakkara, C. Gunathilake, R. Dassanayake, Suitability of reusing the spent diatomaceous earth in brick production: a review, *Adv. Technol.* 2 (2022) 151–166, <https://doi.org/10.31357/ait.v2i2.5529>.
- [34] N. Degirmenci, A. Yilmaz, Use of diatomite as partial replacement for Portland cement in cement mortars, *Constr. Build. Mater.* 23 (2009) 284–288, <https://doi.org/10.1016/j.conbuildmat.2007.12.008>.
- [35] E.J. Vandamme, S. De Baets, A. Vanbaelen, K. Joris, P. De Wulf, Improved production of bacterial cellulose and its application potential, *Polym. Degrad. Stab.* 59 (1998) 93–99, [https://doi.org/10.1016/S0141-3910\(97\)00185-7](https://doi.org/10.1016/S0141-3910(97)00185-7).
- [36] Z. Basaran Bundur, M.J. Kirisits, R.D. Ferron, Biomineralized cement-based materials: Impact of inoculating vegetative bacterial cells on hydration and strength, *Cem. Concr. Res.* 67 (2015) 237–245, <https://doi.org/10.1016/j.cemconres.2014.10.002>.
- [37] K.K. Sahoo, A.K. Sathyan, C. Kumari, P. Sarkar, R. Davis, Investigation of cement mortar incorporating *Bacillus sphaericus*, *Int. J. Smart Nano Mater.* 7 (2016) 91–105, <https://doi.org/10.1080/19475411.2016.1205157>.
- [38] S. Basha, L.K. Lingamgunta, J. Kannali, S.K. Gajula, R. Bandikari, S. Dasari, V. Dalavai, P. Chinthala, P.B. Gundala, P. Kutagolla, V.K. Balaji, Subsurface endospore-forming bacteria possess bio-sealant properties, *Sci. Rep.* 8 (2018) 1–13, <https://doi.org/10.1038/s41598-018-24730-3>.
- [39] C.-M. Aldea, W.-J. Song, J.S. Popovics, S.P. Shah, Extent of healing of cracked normal strength concrete, *J. Mater. Civ. Eng.* 12 (2000) 92–96, [https://doi.org/10.1061/\(asce\)0899-1561\(2000\)12:1\(92\)](https://doi.org/10.1061/(asce)0899-1561(2000)12:1(92)).
- [40] M. Şahmaran, İ.Ö. Yaman, Influence of transverse crack width on reinforcement corrosion initiation and propagation in mortar beams, *Can. J. Civ. Eng.* 35 (2008) 236–245, <https://doi.org/10.1139/L07-117>.
- [41] J.Y. Wang, H. Soens, W. Verstraete, N. De Belie, Self-healing concrete by use of microencapsulated bacterial spores, *Cem. Concr. Res.* 56 (2014) 139–152, <https://doi.org/10.1016/j.cemconres.2013.11.009>.
- [42] W. Khaliq, M.B. Ehsan, Crack healing in concrete using various bio influenced self-healing techniques, *Constr. Build. Mater.* 102 (2016) 349–357, <https://doi.org/10.1016/j.conbuildmat.2015.11.006>.
- [43] V. Wiktor, H.M. Jonkers, Quantification of crack-healing in novel bacteria-based self-healing concrete, *Cem. Concr. Compos.* 33 (2011) 763–770, <https://doi.org/10.1016/j.cemconcomp.2011.03.012>.
- [44] K. Vijay, M. Murmu, S.V. Deo, Bacteria based self healing concrete – A review, *Constr. Build. Mater.* 152 (2017) 1008–1014, <https://doi.org/10.1016/j.conbuildmat.2017.07.040>.
- [45] M.V.S. Rao, V.S. Reddy, C. Sasikala, Performance of microbial concrete developed using *Bacillus subtilis* Jc3, *J. Inst. Eng. Ser. A.* 98 (2017) 501–510, <https://doi.org/10.1007/s40030-017-0227-x>.
- [46] B. Savija, E. Schlangen, Autogeneous healing and chloride ingress in cracked concrete, *Heron.* 61 (2016) 15–32.
- [47] M. Ismail, A. Toumi, R. François, R. Gagné, Effect of crack opening on the local diffusion of chloride in cracked mortar samples, *Cem. Concr. Res.* 38 (2008) 1106–1111, <https://doi.org/10.1016/j.cemconres.2008.03.009>.
- [48] M. Maes, D. Snoeck, N. De Belie, Chloride penetration in cracked mortar and the influence of autogenous crack healing, *Constr. Build. Mater.* 115 (2016) 114–124, <https://doi.org/10.1016/j.conbuildmat.2016.03.180>.
- [49] H. Doostkami, M. Roig-Flores, P. Serna, Self-healing efficiency of Ultra High-Performance Fiber-Reinforced Concrete through permeability to chlorides, *Constr. Build. Mater.* 310 (2021), 125168, <https://doi.org/10.1016/j.conbuildmat.2021.125168>.
- [50] V. Achal, A. Mukerjee, M. Sudhakra Reddy, Biogenic treatment improves the durability and remediates the cracks of concrete structures, *Constr. Build. Mater.* 48 (2013) 1–5, <https://doi.org/10.1016/j.conbuildmat.2013.06.061>.
- [51] N. Chahal, R. Siddique, A. Rajor, Influence of bacteria on the compressive strength, water absorption and rapid chloride permeability of concrete incorporating silica fume, *Constr. Build. Mater.* 37 (2012) 645–651, <https://doi.org/10.1016/j.conbuildmat.2012.07.029>.
- [52] A. Negrini, M. Roig-Flores, E.J. Mezquida-Alcaraz, L. Ferrara, P. Serna, M. G. Grantham, C. Mircea, Effect of crack pattern on the self-healing capability in traditional, HPC and UHPFRC concretes measured by water and chloride permeability, *MATEC Web Conf.* 289 (2019) 01006.

- [53] J.P. Charron, E. Denarié, E. Brühwiler, Permeability of ultra high performance fiber reinforced concretes (UHPPFRC) under high stresses, *Mater. Struct. Constr.* 40 (2007) 269–277, <https://doi.org/10.1617/s11527-006-9105-0>.
- [54] F. Lo Monte, L. Ferrara, Self-healing characterization of UHPPFRC with crystalline admixture: Experimental assessment via multi-test/multi-parameter approach, *Constr. Build. Mater.* 283 (2021), 122579, <https://doi.org/10.1016/j.conbuildmat.2021.122579>.
- [55] C. Litina, G. Bumanis, G. Anglani, M. Dudek, R. Maddalena, M. Amenta, S. Papaioannou, G. Pérez, J.L. García Calvo, E. Asensio, R. Beltrán Cobos, F. Tavares Pinto, A. Augonis, R. Davies, A. Guerrero, M. Sánchez Moreno, T. Stryzewska, I. Karatasios, J.-M. Tulliani, P. Antonaci, D. Bajare, A. Al-Tabbaa, Evaluation of methodologies for assessing self-healing performance of concrete with mineral expansive agents: An interlaboratory study, *Materials (Basel)* 14 (8) (2021) 2024.
- [56] H. Doostkami, S. Formagini, J.E. Cumberbatch, M. Roig-Flores, P. Serna, Self-healing capability of conventional and high-performance concrete containing SAP by means of water permeability, *Fib Int. Congr. 2022 Oslo*. (2022).
- [57] H. Doostkami, J. de Jesús Estacio Cumberbatch, S. Formagini, M. Roig-Flores, P. Serna, M.G. Grantham, M. Basheer, R. Mangabhai, Self-healing of concrete containing commercial bacteria by means of water and chlorides permeability, *MATEC Web Conf.* 361 (2022) 05010.
- [58] N. Otsuki, S. Nagataki, K. Nakashita, Evaluation of the AgNO₃ solution spray method for measurement of chloride penetration into hardened cementitious matrix materials, *Constr. Build. Mater.* 7 (1993) 195–201, [https://doi.org/10.1016/0950-0618\(93\)90002-T](https://doi.org/10.1016/0950-0618(93)90002-T).
- [59] M. Collepardi, 2 Quick Method To Determine Free and Bound Chloride in concrete, *Dep. Sci. Mater. Earth, Univ. Ancona, Italy*. 10 (1995) 10–16.
- [60] F. He, C. Shi, Q. Yuan, C. Chen, K. Zheng, AgNO₃-based colorimetric methods for measurement of chloride penetration in concrete, *Constr. Build. Mater.* 26 (2012) 1–8, <https://doi.org/10.1016/j.conbuildmat.2011.06.003>.
- [61] M. Collepardi, 2 Quick method to determine free and bound chlorides in concrete, in: *RILEM Int. Work. Chloride Penetration into Concr.*, RILEM Publications SARL, 1995: pp. 10–16. <https://doi.org/10.1617/2912143454.002>.
- [62] E. Meck, V. Sirivivatnanon, Field indicator of chloride penetration depth, *Cem. Concr. Res.* 33 (2003) 1113–1117, [https://doi.org/10.1016/S0008-8846\(03\)00012-7](https://doi.org/10.1016/S0008-8846(03)00012-7).
- [63] C. Tasdemir, M.A. Tasdemir, F.D. Lydon, B.I.G. Barr, Effects of silica fume and aggregate size on the brittleness of concrete, *Cem. Concr. Res.* 26 (1996) 63–68, [https://doi.org/10.1016/0008-8846\(95\)00180-8](https://doi.org/10.1016/0008-8846(95)00180-8).
- [64] A. Yan, K.R. Wu, D. Zhang, W. Yao, Effect of fracture path on the fracture energy of high-strength concrete, *Cem. Concr. Res.* 31 (2001) 1601–1606, [https://doi.org/10.1016/S0008-8846\(01\)00610-X](https://doi.org/10.1016/S0008-8846(01)00610-X).
- [65] S. Hou, K. Li, Z. Wu, F. Li, C. Shi, Quantitative evaluation on self-healing capacity of cracked concrete by water permeability test – A review, *Cem. Concr. Compos.* 127 (2022) 104404.
- [66] H.L. Wang, J.G. Dai, X.Y. Sun, X.L. Zhang, Characteristics of concrete cracks and their influence on chloride penetration, *Constr. Build. Mater.* 107 (2016) 216–225, <https://doi.org/10.1016/j.conbuildmat.2016.01.002>.
- [67] J.P. Charron, E. Denarié, E. Brühwiler, Transport properties of water and glycol in an ultra high performance fiber reinforced concrete (UHPPFRC) under high tensile deformation, *Cem. Concr. Res.* 38 (2008) 689–698, <https://doi.org/10.1016/j.cemconres.2007.12.006>.
- [68] R. Roy, E. Rossi, J. Silfwerbrand, H. Jonkers, Self-healing capacity of mortars with added-in bio-plastic bacteria-based agents: Characterization and quantification through micro-scale techniques, *Constr. Build. Mater.* 297 (2021), 123793, <https://doi.org/10.1016/j.conbuildmat.2021.123793>.
- [69] P. Ecoffres, C. Desmettre, J.P. Charron, Effect of a crystalline admixture on the self-healing capability of high-performance fiber reinforced concretes in service conditions, *Constr. Build. Mater.* 173 (2018) 763–774, <https://doi.org/10.1016/j.conbuildmat.2018.04.003>.
- [70] B. Xi, S. Al-Obaidi, L. Ferrara, Effect of different environments on the self-healing performance of Ultra High-Performance Concrete – A systematic literature review, *Constr. Build. Mater.* 374 (2023), 130946, <https://doi.org/10.1016/j.conbuildmat.2023.130946>.
- [71] Y.S. Lee, W. Park, Current challenges and future directions for bacterial self-healing concrete, *Appl. Microbiol. Biotechnol.* 102 (2018) 3059–3070, <https://doi.org/10.1007/s00253-018-8830-y>.
- [72] M. Heng, K. Murata, Aging of concrete buildings and determining the pH value on the surface of concrete by using a handy semi-conductive pH meter, *Anal. Sci.* 20 (2004) 1087–1090, <https://doi.org/10.2116/analsci.20.1087>.
- [73] J. Feng, B. Chen, W. Sun, Y. Wang, Microbial induced calcium carbonate precipitation study using *Bacillus subtilis* with application to self-healing concrete preparation and characterization, *Constr. Build. Mater.* 280 (2021) 122460.
- [74] J. Wang, H.M. Jonkers, N. Boon, N. De Belie, *Bacillus sphaericus* LMG 22257 is physiologically suitable for self-healing concrete, *Appl. Microbiol. Biotechnol.* 101 (2017) 5101–5114, <https://doi.org/10.1007/s00253-017-8260-2>.
- [75] D. Zhang, M.A. Shahin, Y. Yang, H. Liu, L. Cheng, Effect of microbially induced calcite precipitation treatment on the bonding properties of steel fiber in ultra-high performance concrete, *J. Build. Eng.* 50 (2022), 104132, <https://doi.org/10.1016/j.jobe.2022.104132>.
- [76] Q. Yuan, D. Deng, C. Shi, G. de Schutter, Application of silver nitrate colorimetric method to non-steady-state diffusion test, *J. Cent. South Univ.* 19 (2012) 2983–2990, <https://doi.org/10.1007/s11771-012-1367-9>.
- [77] Q. Yuan, C. Shi, F. He, G. De Schutter, K. Audenaert, K. Zheng, Effect of hydroxyl ions on chloride penetration depth measurement using the colorimetric method, *Cem. Concr. Res.* 38 (2008) 1177–1180, <https://doi.org/10.1016/j.cemconres.2008.04.003>.
- [78] V. Baroghel-Bouny, P. Belin, M. Maultzsch, D. Henry, AgNO₃ spray tests: advantages, weaknesses, and various applications to quantify chloride ingress into concrete. Part 1: Non-steady-state diffusion tests and exposure to natural conditions, *Mater. Struct.* 40 (2007) 759–781, <https://doi.org/10.1617/s11527-007-9233-1>.